Angle-resolved photoabsorption spectra of core holes with strong spin-orbit interaction: Below the Br 3*d* thresholds in HBr

R. Püttner,[1,2] Y.-F. Hu,[3] E. Nõmmiste,[1,4] G. M. Bancroft,[3] and S. Aksela[1]
[1]*University of Oulu, Department of Physical Sciences, P.O. Box 3000, 90401 Oulu, Finland*
[2]*Freie Universität Berlin, Institute for Experimental Physics, Arnimallee 14, D-14195 Berlin, Germany*
[3]*Department of Chemistry, The University of Western Ontario, London, Ontario, Canada N6A 5B7*
[4]*Institute of Physics, University of Tartu, Tartu 51014, Estonia*
(Received 16 October 2000; published 27 February 2002)

High-resolution angle-resolved photoabsorption spectra of HBr below the Br 3*d* ionization thresholds were recorded in the total ion yield. By applying adequate selection rules for excitations from core holes with a strong spin-orbit interaction, we demonstrate for the $3d^{-1}_{j,m_j}nl\lambda$ states that this technique is a powerful tool to study the multiplet splitting of the Rydberg states into the different sublevels M_j. We report a multiplet splitting of $\cong 50$ meV between the $M_j=1$ and 0^+ substates of the $3d^{-1}_{5/2,1/2}5s\sigma$ and $3d^{-1}_{3/2,1/2}5s\sigma$ excitations. As a consequence of this observation, an assignment of the photoabsorption spectrum different to those of earlier studies is derived in the low-energy region. In addition, the orientation parameter β_m is derived from the spectra.

DOI: 10.1103/PhysRevA.65.032513 PACS number(s): 33.20.Ni, 33.15.Pw, 33.15.Ry, 33.80.Eh

I. INTRODUCTION

In core-level spectroscopy the excitation and deexcitation processes occur at a time scale that is short as compared to the time scale of the molecular rotation. The final states of the dominating decay process, namely, the Auger process, predominantly possess potential-energy curves which are not stable with respect to dissociation, hence diatomic molecules dissociate along their molecular axis, which can be considered as fixed in space during the entire process. As a consequence, the detection of the fragment ions in any particular direction can be employed to obtain information about the spatial orientation of the molecule during the process. Combining this information with the polarization vector of the light source, one can apply more specific selection rules in order to assign the spectra.

This effect has been used for a number of 1*s* excitations in linear molecules consisting of first-row elements, e.g., N_2, since the fundamental work of Yagishita *et al.* [1]. For 1*s* excitations the more specific selection rules are $\Delta\Lambda=\pm 1$ for the $\theta=90°$ spectra and $\Delta\Lambda=0$ for the $\theta=0°$ spectra by defining θ as the angle between the polarization vector of the light and the direction of detection. Consequently, for $1s\sigma$ core levels only excitations into $nl\sigma$ and $nl\pi$ states can be observed in the $\theta=0°$ and $\theta=90°$ spectra, respectively.

However, by creating core holes with nonvanishing angular momenta, e.g., *np* or *nd* holes, spin-orbit interaction becomes important. As a consequence, the orbital angular momentum of these core holes is no longer a good quantum number and no information similar to the ones for 1*s* excitations can be obtained from the spectra. Up to now only a limited amount of work has been performed on angle-resolved photoabsorption spectra of molecules containing second-row elements, e.g., HCl [2].

The electronic structure of HBr below the Br 3*d* ionization threshold was first studied by Shaw *et al.* [3] using electron-impact excitation. They only considered spin-orbit splitting, but neglected ligand-field splitting, leading to a number of inconsistencies between the data and the proposed assignment. In the early 1990s Liu *et al.* [4] showed that the ligand-field splitting is an important effect in the photoelectron spectroscopic study of the Br 3*d* level in HBr. This led to a reassignment of the photoabsorption spectra [5,6] and to a subsequent support of the assignment in its main ideas by resonant Auger spectroscopy [7].

In a recent theoretical study by Fink *et al.* [8], it was shown for the $2p\rightarrow$ Rydberg excitations in HCl that $2p^{-1}_{j,m_j}nl\lambda$ is a good description of the final states. These $2p^{-1}_{j,m_j}nl\lambda$ configurations are subject to a multiplet splitting into different M_j values and only the states with $M_j=0^+(1)$ can be observed in the $0°(90°)$ spectra. In the present work, we describe the Rydberg states with $3d^{-1}_{j,m_j}nl\lambda$ and demonstrate how the concept of selection rules for angle-resolved spectra can be extended to *np* and *nd* core levels in order to derive information for the assignment. More importantly we show that the technique of angle-resolved spectra is well suited to study the multiplet splitting of the Rydberg states into the different sublevels M_j. We report multiplet splitting of $\cong 50$ meV between the sublevels $M_j=0^+$ and 1 for the $3d^{-1}_{5/2,1/2}5s\sigma$ and $3d^{-1}_{3/2,1/2}5s\sigma$ states. A splitting of the same amount was recently also predicted by theory for the $2p^{-1}_{3/2,1/2}4s\sigma$ and $2p^{-1}_{1/2,1/2}4s\sigma$ states in HCl [8]. It is clear that a multiplet splitting of this order of magnitude has to be considered for a correct assignment of integrated core-level photoabsorption spectra in general. For example, the splitting of the Br $3d^{-1}_{5/2,1/2}5s\sigma$ resonance is clearly observed in angular integrated photoabsorption spectra [5,6]. However, with this multiplet splitting neglected, these resonances were incorrectly assigned to $3d^{-1}_{5/2}4d\pi$, which was also supported by multiple scattering-X_α (MS-X_α) calculations [4]. Using the angle-resolved photoabsorption spectra, the molecular orientation parameter β_m was determined.

TABLE I. Coupling scheme of np and nd core hole states with $nl\lambda$ Rydberg electrons. The M_j values that can be populated from the ground state on the basis of dipole-selection rules are indicated in bold.

σ-like Rydberg orbital ($l_z=0$)			
j_z	5/2	3/2	1/2
$K_z = j_z \pm l_z$	5/2	3/2	1/2
$M_j = K_z \pm s_z$	3,2	2,**1**	**1,0$^+$**,0$^-$
π-like Rydberg orbital ($l_z=1$)			
j_z	5/2	3/2	1/2
$K_z = j_z \pm l_z$	7/2;3/2	5/2;1/2	3/2;1/2
$M_j = K_z \pm s_z$	4,3;2,**1**	3,2;**1,0$^+$**,0$^-$	2,**1;1,0$^+$**,0$^-$
δ-like Rydberg orbital ($l_z=2$)			
j_z	5/2	3/2	1/2
$K_z = j_z \pm l_z$	9/2;1/2	7/2;1/2	3/2;1/2
$M_j = K_z \pm s_z$	5,4;**1,0$^+$**,0$^-$	4,3;**1,0$^+$**,0$^-$	2,**1;1,0$^+$**,0$^-$

This parameter is important to understand the β parameters of resonant Auger transitions in molecules.

II. EXPERIMENT AND DATA ANALYSIS

The measurements were performed at the MAX I storage ring in Lund, Sweden using the ''Finnish beamline'' BL 51 [9]. The beamline was operated at a short-period undulator [10] and the radiation was monochromatized by a SX700 plane grating monochromator [11]. The angle-resolved photoabsorption spectra were measured detecting the total ion yield induced by radiation in the photon energy range of $\cong$69–79 eV. The ion yield was measured with a time of flight (TOF) spectrometer (field free drift tube length 106 mm) connected to the rotatable spectrometer chamber, which also includes the Scienta-200 electron spectrometer for measuring angle-resolved electron spectra. The spectra were taken at $\theta=0°$ and 90° with respect to the polarization direction of the light. Due to some penetration of the accelerating field into the source volume, it turned out that the TOF system has a rather wide angle of acceptance, which leads to considerable contribution of a $\theta=90°$ spectrum in a $\theta=0°$ spectrum and vice versa. To eliminate the respective unwanted contributions in the angle-resolved spectra, a procedure based on the assignment of the nonoverlapping peak at 74.590 eV to $3d^{-1}_{5/2,5/2}5p\pi$ [5,6] was applied. This resonance is expected to show no contributions in the $\theta=0°$ spectrum since it possesses no $M_j=0^+$ sublevel (see below). Therefore a weighted $\theta=90°$ spectrum was subtracted from the $\theta=0°$ spectrum in order to eliminate all contributions from this resonance. The pure $\theta=0°$ spectrum was then weighted accordingly and subtracted from the $\theta=90°$ spectrum. The results obtained were checked by adding two times the 90° spectrum and one time the 0° spectrum in order to confirm the treatment of the spectra by comparing the result with the well-known 55° spectrum [5,6]. The normalized spectra were fitted with Lorentzian line shapes using a width of $\Gamma \cong 95$ meV to describe the lifetime broadening [5] and convoluted with a Gaussian line shape of $\cong 30$ meV to simulate the experimental resolution.

III. THE ANGLE-RESOLVED PHOTABSORPTION SPECTRA

A. Selection rules and coupling schemes

By considering spin-orbit interaction, the adequate selection rules for photoabsorption spectra are $\Delta M_j=0$ or ± 1. For angle-resolved photoabsorption spectra, these selection rules can be specified as

$$\Delta M_j = \pm 1 \quad \text{for} \quad \theta=90° \quad \text{and} \quad \Delta M_j = 0 \quad \text{for} \quad \theta=0°, \tag{1}$$

i.e., only $M_j=0^+$ and 1 states can be observed in the 0° and 90° spectra, respectively. This can be exploited to help assigning the normal photoabsorption spectra by determining the possible M_j values for the $3d^{-1}_{j,j_z}nl\lambda$ Rydberg excitations. To do this, first j_z of the core hole has to be coupled to the z component of the orbital momentum l_z of the Rydberg orbital with $l_z=0,1,2$, etc., for $\lambda=\sigma$, π, and δ-like Rydberg orbitals, respectively. The rule for adding the z component of the angular momentum is $K_z = j_z \pm l_z$. Second, by coupling K_z to the spin s_z of the Rydberg electron one gets $M_j = K_z \pm s_z$. A detailed coupling scheme for np and nd core holes with $nl\lambda$ Rydberg states is given in Table I. Note that each different symmetry of the Rydberg orbital (σ,π,δ) shows its characteristic pattern in the angle-resolved photoabsorption spectrum, e.g., a σ-like Rydberg orbital can contribute in the $\theta=90°$ spectra with excitations originating from the $nd^{-1}_{5/2,3/2}$, $nd^{-1}_{5/2,1/2}$, $nd^{-1}_{3/2,3/2}$, and $nd^{-1}_{3/2,1/2}$ ligand-field component of the core hole; however, it can contribute in the $\theta=0°$ spectra only for the excitations from the $nd^{-1}_{5/2,1/2}$ and $nd^{-1}_{3/2,1/2}$ ligand-field component.

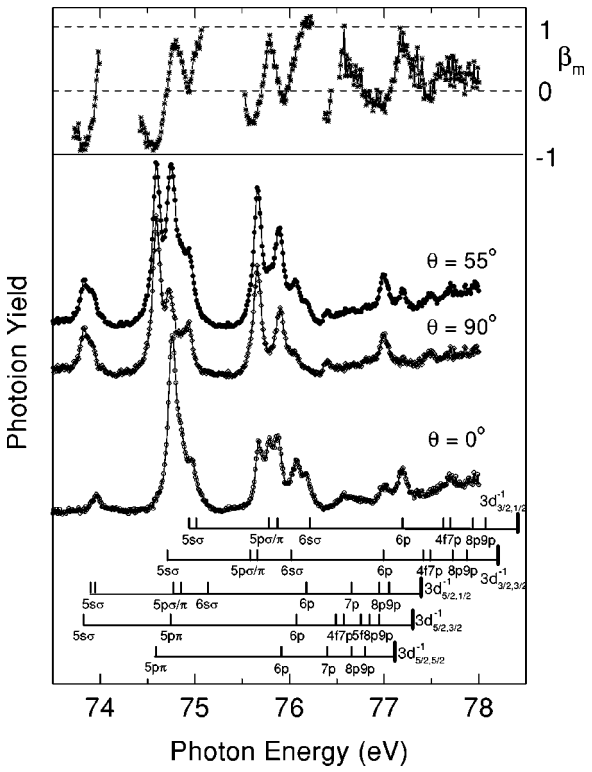

FIG. 1. Angle-resolved photoabsorption spectra for $\theta=0°$ (hollow circles) and $\theta=90°$ (hollow diamonds) as well as a ''calculated'' spectrum for $\theta=55°$ (filled circles). The assignment is given by the bar diagrams in the lower part of the figure. The upper part of the figure displays the orientation parameter β_m.

B. Angle-resolved photoabsorption spectra

Figure 1 shows the angle-resolved photoabsorption spectra of HBr for $\theta=0°$ and $\theta=90°$. Considerable differences are seen between these different spectra, especially in the lower-energy region up to 76.5 eV where there is less overlap between the Rydberg states. The differences for the spectra measured at different angles are also reflected by the strong variation of the orientation parameter β_m shown in the uppermost part of Fig. 1 (see below). In addition, a ''calculated'' 55° spectrum, i.e., a sum of two times the 90° spectrum plus one times the 0° spectrum, is shown in Fig. 1. This matches very well with the angle-integrated photoabsorption spectra [5,6]. This confirms that the applied procedure eliminates the contributions of the respective unwanted angle.

The assignment based on the present analysis is given in the lower part of Fig. 1. Differences between the present and earlier [5] assignments are only obtained below $h\nu=75.5$ eV. These are mainly related to the $3d\rightarrow 4d\pi$ excitations in Refs. [5,6], which are now reassigned to $3d\rightarrow 5s\sigma$. The assignments for higher Rydberg states are affected only slightly by this reassignment. Above the photon energy $h\nu=75.5$ eV the observations of the present work are in agreement with the earlier assignment of Ref. [5]; the present assignment is adopted due to the higher resolution and the better signal-to-noise ratio in the earlier work. This also holds for a number of resonances that are not observed in the present work, however, clearly identified in the angle-integrated photoabsorption spectra [5].

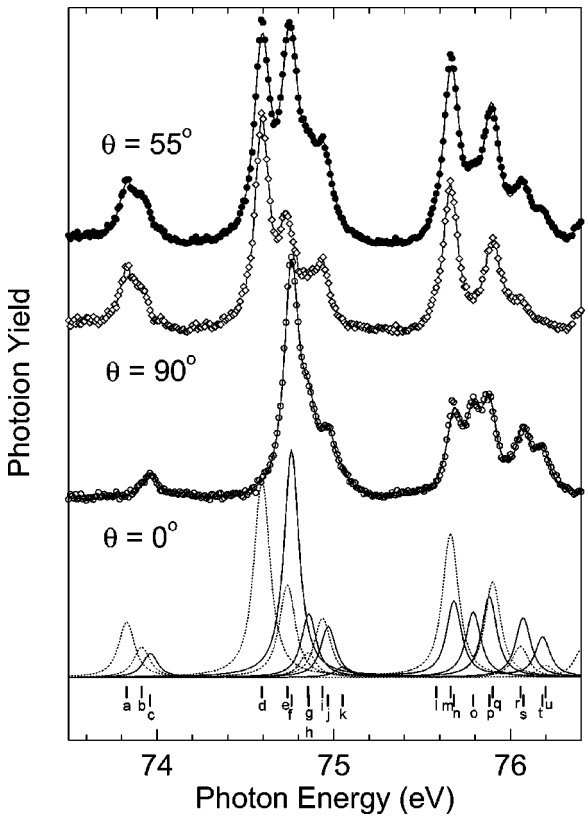

FIG. 2. Angle-resolved photoabsorption spectra for $\theta=0°$ (hollow circles) and $\theta=90°$ (hollow diamonds) as well as a ''calculated'' spectrum for $\theta=55°$ (filled circles) in the energy range from 73.5–76.4 eV. The dashed (solid) subspectra show the states with $M_j=1(M_j=0^+)$. For a detailed assignment see Table II.

Figure 2 shows the lower-energy range in detail. The fitted result is represented by the solid lines through the data points and the solid (dotted) subspectra represent the results for the $\theta=0°(\theta=90°)$ spectrum, i.e., the final states with $M_j=0^+(M_j=1)$. The detailed assignment of the states is given in Table II. Peaks (a)–(c) show a splitting smaller than the ligand-field splitting and an M_j pattern of $1,1,0^+$ (i.e., two peaks with $M_j=1$ observed in the $\theta=90°$ spectrum, and one peak with $M_j=0^+$ when $\theta=0°$). From Table I, we note that a M_j pattern of $1,1,0^+,1,1,0^+$ is expected for excitations into π-like Rydberg orbitals, while an M_j pattern of $1,1,0^+$ is expected for excitations into σ-like Rydberg states. More importantly, the energy separation pattern among peaks (a)–(c) is in agreement with the pattern expected for excitations into σ-like Rydberg states, not π-like Rydberg states. Specifically, the energy splitting between peak (a) and peak (c) of $\cong 130$ meV is much smaller than the ligand-field splitting between the $3d^{-1}_{5/2,5/2}$ and $3d^{-1}_{5/2,1/2}$ core-hole states of $\cong 275$ meV [5,6]. However, the energy splitting between peak (a) and the mean energy value of peaks (b) and (c) of $\cong 110$ meV agrees well with the ligand-field splitting between the $3d^{-1}_{5/2,3/2}$ and $3d^{-1}_{5/2,1/2}$ core holes [5,6]. This small experimental splitting can be explained with the assignment of a $nl\sigma$ Rydberg state, since the $3d^{-1}_{5/2,5/2}nl\sigma$ excitation is dipole forbidden. However, this experimental

TABLE II. The assignment of the Rydberg states below $\hbar\nu = 76.2$ eV.

Peak	Energy (eV)	Assignment
(*a*)	73.828	$3d^{-1}_{5/2,3/2}5s\sigma \;\; M_j=1$
(*b*)	73.913	$3d^{-1}_{5/2,1/2}5s\sigma \;\; M_j=1$
(*c*)	73.962	$3d^{-1}_{5/2,1/2}5s\sigma \;\; M_j=0^+$
(*d*)	74.594	$3d^{-1}_{5/2,5/2}5p\pi \;\; M_j=1$
(*e*)	74.737	$3d^{-1}_{3/2,3/2}5s\sigma \;\; M_j=1$ and $3d^{-1}_{5/2,3/2}5p\sigma \;\; M_j=1$
(*f*)	74.761	$3d^{-1}_{5/2,3/2}5p\pi \;\; M_j=0^+$ and $3d^{-1}_{5/2,1/2}5p\sigma \;\; M_j=0^+$
(*g*)	74.854	$3d^{-1}_{5/2,1/2}5p\pi \;\; M_j=1$
(*h*)	74.859	$3d^{-1}_{5/2,3/2}5p\pi \;\; M_j=0^+$
(*i*)	74.936	$3d^{-1}_{3/2,1/2}5s\sigma \;\; M_j=1$
(*j*)	74.968	$3d^{-1}_{3/2,1/2}5s\sigma \;\; M_j=0^+$
(*k*)	75.050	$3d^{-1}_{5/2,1/2}6s\sigma \;\; M_j=0^+$
(*l*)	75.580	$3d^{-1}_{3/2,3/2}5p\sigma \;\; M_j=1$
(*m*)	75.661	$3d^{-1}_{3/2,3/2}5p\pi \;\; M_j=1$
(*n*)	75.680	$3d^{-1}_{3/2,3/2}5p\pi \;\; M_j=0^+$
(*o*)	75.789	$3d^{-1}_{3/2,1/2}5p\sigma \;\; M_j=0^+$
(*p*)	75.880	$3d^{-1}_{3/2,1/2}5p\pi \;\; M_j=0^+$
(*q*)	75.900	$3d^{-1}_{3/2,1/2}5p\pi \;\; M_j=1$ and $3d^{-1}_{5/2,5/2}6p\pi \;\; M_j=1$
(*r*)	76.056	$3d^{-1}_{5/2,3/2}6p \;\; M_j=1$
(*s*)	76.072	$3d^{-1}_{5/2,3/2}6p \;\; M_j=0^+$
(*t*)	76.182	$3d^{-1}_{5/2,1/2}6p \;\; M_j=0^+$
(*u*)	76.199	$3d^{-1}_{5/2,1/2}6p \;\; M_j=1$

splitting is too small for the assignment of a $nl\pi$ Rydberg state, since excitations originating from all three components of the $3d_{5/2}$ core hole are dipoleallowed and a splitting in the order of $\cong 275$ meV is expected between peaks (*a*) and (*c*). From this we conclude the resonances (*a*)–(*c*) to be excitations into a σ-like orbital instead of a $4d\pi$ Rydberg orbital, which was preferred in previous assignments [5,6]. This reassignment is supported by the results of resonant Auger spectroscopy [12]. In particular, we assign resonances (*a*)–(*c*) to $3d^{-1}_{5/2,3/2}5s\sigma \;\; M_j=1$, $3d^{-1}_{5/2,1/2}5s\sigma \;\; M_j=1$, and $3d^{-1}_{5/2,1/2}5s\sigma \;\; M_j=0^+$, respectively.

In addition to the above $5s\sigma$ assignment, peaks (*a*)–(*c*) could also be assigned to resonances from excitations into the $4d\sigma$ Rydberg orbital, on the basis of the M_j pattern argument alone. However, a large multiplet splitting of $\cong 50$ meV between peaks (*b*) and (*c*) is consistent with the fact that the multiplet splitting between $3d^{-1}_{5/2,1/2}5s\sigma \;\; M_j=1$ and 0^+ states is much larger than the splitting between $3d^{-1}_{5/2,1/2}4d\sigma \;\; M_j=1$ and 0^+ states due to the relatively high vicinity of the core hole and the $5s\sigma$ Rydberg state. Theoretical values for this multiplet splitting in the corresponding excitations $2p^{-1}_{3/2,1/2}4s\sigma$ and $2p^{-1}_{3/2,1/2}3d\sigma$ of HCl are reported to be $\cong 60$ meV and $\cong 17$ meV, respectively [8], in agreement with our conclusions. The assignment of the first state to an excitation from the $3d^{-1}_{5/2,3/2}$ core hole and the well-known values for the spin-orbit and ligand-field splitting [5,6] leads to the assignment of peak (*e*) to $3d^{-1}_{3/2,3/2}5s\sigma \;\; M_j=1$, maybe overlapping with $3d^{-1}_{5/2,3/2}5p\sigma \;\; M_j=1$ contributions, as well as peaks (*i*) and (*j*) to $3d^{-1}_{3/2,1/2}5s\sigma \;\; M_j=1$ and $3d^{-1}_{3/2,1/2}5s\sigma \;\; M_j=0^+$, respectively. Assigning peak (*e*) at least partly to $3d^{-1}_{3/2,3/2}5s\sigma \; M_j=1$ is supported by resonant Auger spectra since the typical lines subsequent to a $3d\rightarrow 5s$ excitation are present at these photon energies [12]; this finding in the resonant Auger spectra [12] could not be explained with the previous assignment of the photoabsorption spectra [5,6]. This reassignment also shows that the MS-$X\alpha$ calculations presented in Ref. [4] were not adequate to describe the intensities of the Br $3d\rightarrow$ Rydberg excitations correctly since they predict an almost vanishing oscillator strength for the $3d\rightarrow 5s\sigma$ Rydberg excitation.

The present reassignment leads to a quantum defect $\delta_{5s} \cong 3$ and requires a reconsideration of the peaks labeled in Fig. 1 as excitations into $6s\sigma$ Rydberg orbitals. The latter excitations result in a quantum defect $\delta_{6s} \cong 3.5$, which is approximately 15% larger than the one for the $3d\rightarrow 5s$ excitations. This large increase in the quantum defect is not in line with the concept of constant quantum defects for a given Rydberg series $nl\lambda$ of the molecule. However, it does not necessarily reject the assignment to $3d\rightarrow 6s$ excitations since a similar amount of increase in the quantum defect was also observed experimentally and theoretically for the two lowest states of the O $1s^{-1}ns$ Rydberg excitations in CO and NO [13,14]. An alternative reassignment of the $3d\rightarrow 6s$ resonances to $3d\rightarrow 4d$ excitations would lead to a quantum defect $\delta_{4d} \cong 1.5$, which would be in good agreement with the quantum defect $\delta_{4d} \cong 1.3$ for the $3d\rightarrow 4d$ excitations in isoelectronic Kr [15]; the difference of 0.2 in the quantum defect can be explained by the reduction of the symmetry from Kr to HBr. This symmetry reduction would lead to a splitting of the $3d^{-1}4d$ Rydberg states in Kr into the sublevels $3d^{-1}4d\sigma$, $3d^{-1}4d\pi$, and $3d^{-1}4d\delta$ in HBr, and, consequently, to a shift in the energy positions and quantum defects for at least some of the $4d$ levels. It has been shown for HCl that this splitting is much larger for the corresponding $2p\rightarrow 3d$ excitations than that for the $2p\rightarrow 4p$ excitations. As a consequence of the present discussion, a final assignment cannot be given based on the quantum-defect argument. The earlier assignment of the higher $3d\rightarrow np$ and nf states [5] remain unaffected from the reassignment in the low-energy region of the spectrum.

C. The orientation parameter β_m

In a two-step model, i.e., by considering the photoexcitation and the subsequent resonant Auger process separately, the angular asymmetry parameter β of the molecular Auger decay can be factorized as [16]

$$\beta = \beta_m \alpha_2, \tag{2}$$

where α_2 represents the intrinsic anisotropy parameter of the Auger decay and β_m describes the spacial orientation of the axis of a linear molecule. In the axial-recoil approximation β_m can be determined according to [17]

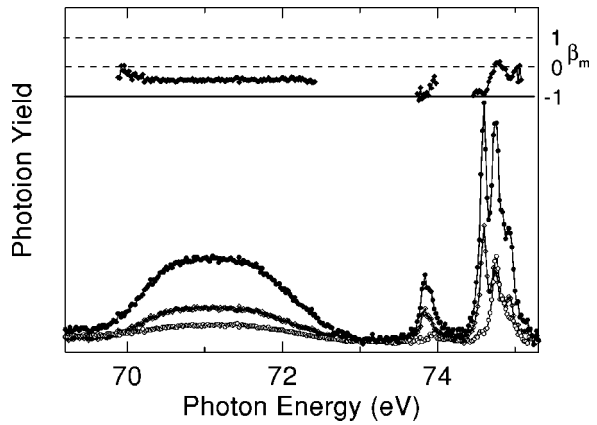

FIG. 3. Angle-resolved photoabsorption spectra for $\theta=0°$ (hollow circles) and $\theta=90°$ (hollow diamonds) as well as a ''calculated'' spectrum for $\theta=55°$ (filled circles) in the energy range of the $3d\rightarrow\sigma^*$ excitations. The upper part of the figure displays the orientation parameter β_m.

$$\beta_m=\frac{2(D_\parallel^2-D_\perp^2)}{D_\parallel^2+2D_\perp^2}. \tag{3}$$

$D_\parallel^2(D_\perp^2)$ describes the photoabsorption strength parallel (perpendicular) to the electric-field vector.

The spacial orientation parameter β_m is shown for the $3d\rightarrow$ Rydberg excitations in Fig. 1 and for the $3d\rightarrow\sigma^*$ excitations in Fig. 3. In Fig. 1 the errors of the values for β_m are estimated to be ±0.2 for the most intense peaks, however, to be larger for the shoulders and less intense peaks with up to ±0.4. Due to the poorer statistics and larger step size in Fig. 3, we estimate the errors for the excitation into the Rydberg states to ±0.5 and the excitations into the σ^* valence orbital to ±0.3.

In principle, for excitations into final states with $M_j=0^+$ and $M_j=1$ values are $\beta_m=2$ and $\beta_m=-1$, respectively. This can be seen, e.g., for the $3d_{5/2,3/2}5s\sigma$ and $3d_{5/2,5/2}5p\pi$ excitation for which only $M_j=1$ components can be observed. In the energy region of these excitations $\beta_m=-1$. For all other energy regions, the value of β_m is between -1 and 1 due to the overlap of excitations into different Rydberg states or the same Rydberg state, however, with different M_j values.

IV. SUMMARY AND CONCLUSION

In this work we presented angle-resolved photoabsorption spectra of HBr below the Br $3d$ ionization thresholds. Adequate selection rules for the excitations from the Br $3d$ core holes with strong spin-orbit interaction were applied to the angle-resolved spectra. We demonstrated that this method is well suited to study the multiplet splitting of the Rydberg states $3d_{j,m_j}^{-1}nl\lambda$ into the different sublevels M_j. More importantly we report a splitting of $\cong50$ meV between the sublevels $M_j=0^+$ and 1 of the $3d_{5/2,1/2}^{-1}5s\sigma$ excitation, which resulted in a reassignment of the low-energy region of the spectrum. This splitting of $\cong50$ meV has been observed earlier in angle integrated photoabsorption spectra [5,6], however, interpreted incorrectly. The present results show that for the lowest core to Rydberg excitations this splitting has to be taken into consideration for the assignment of photoabsorption spectra of small molecules in general. For example, based on the present findings we suggest a similar reassignment of Br $3d^{-1}4d\pi$ levels to $3d^{-1}5s\sigma$ in the angular integrated Br $3d$ photoabsorption spectrum of Br_2, which is very similar to the spectrum of HBr [6]. From the angle-resolved spectra, we calculated the molecular orientation parameter β_m which is a prerequisite for understanding the angular distribution of the electrons in resonant Auger spectroscopy.

ACKNOWLEDGMENTS

The authors thank Dr. Antti Kivimäki and Dr. Jari Karvonen for discussions and help in the experiment. The staff of the MAX laboratory is gratefully acknowledged for assistance during the measurements. This work has been supported by the Research Council for the Natural Sciences and Engineering of the Academy of Finland and by the Natural Sciences and Engineering Research Council (NSERC) of Canada. The authors thank R. F. Fink for putting results at our disposal prior to publication and for helpful discussions.

[1] A. Yagishita, H. Maezawa, M. Ukai, and E. Shigemasa, Phys. Rev. Lett. **62**, 36 (1989).

[2] E. Shigemase, N. Kosugi, and A. Yagishita (unpublished).

[3] D.A. Shaw, D. Cvejanović, G.C. King, and F.H. Read, J. Phys. B **17**, 1173 (1984).

[4] Z.F. Liu, G.M. Bancroft, K.H. Tan, and M. Schachter, J. Electron Spectrosc. Relat. Phenom. **67**, 299 (1994).

[5] R. Püttner, M. Domke, K. Schulz, A. Gutiérrez, and G. Kaindl, J. Phys. B **28**, 2425 (1995).

[6] J. Johnson, J.M. Cutler, G.M. Bancroft, Y.-F. Hu, and K.H. Tan, J. Phys. B **30**, 4899 (1997).

[7] Y.-F. Hu, G.M. Bancroft, J. Karvonen, E. Nõmmiste, A. Kivimäki, H. Aksela, S. Aksela, and Z.F. Liu, Phys. Rev. A **56**, R3342 (1997).

[8] R.F. Fink, M. Kivilompolo, and H. Aksela, J. Chem. Phys. **111**, 10 034 (1999).

[9] S. Aksela, A. Kivimäki, A. Naves de Brito, O.-P. Sairanen, S. Svensson, and J. Vöyrynen, Rev. Sci. Instrum. **65**, 831 (1994); S. Aksela, A. Kivimäki, O.-P. Sairanen, A. Naves de Brito, E. Nõmmiste, and S. Svensson, *ibid.* **66**, 1621 (1995).

[10] H. Ahola and T. Meinander, Rev. Sci. Instrum. **63**, 372 (1992); Å. Andersson, S. Werin, T. Meinander, A. Naves de Brito, and S. Aksela, Nucl. Instrum. Methods Phys. Res. A **362**, 586 (1995).

[11] R. Nyholm, S. Svensson, J. Nordgren, and A. Foldström, Nucl. Instrum. Methods Phys. Res. A **246**, 267 (1986); S. Aksela, A. Kivimäki, R. Nyholm, and S. Svensson, Rev. Sci. Instrum. **63**, 1252 (1992).

[12] R. Püttner *et al.* (unpublished).
[13] R. Püttner, I. Dominguez, T.J. Morgan, C. Cisneros, R.F. Fink, E. Rotenberg, T. Warwick, M. Domke, G. Kaindl, and A.S. Schlachter, Phys. Rev. A **59**, 3415 (1999).
[14] Y. Zhang, P.-H. Zhang, and J.-M. Li, Phys. Rev. A **56**, 1819 (1997).
[15] G.C. King, M. Tronc, F.H. Read, and R.C. Bradford, J. Phys. B **10**, 2479 (1977).
[16] D. Dill, J.R. Swanson, S. Wallace, and J.L. Dehmer, Phys. Rev. Lett. **45**, 1393 (1980).
[17] J.L. Dehmer and D. Dill, Phys. Rev. A **18**, 164 (1978).